Research Article

Gaohang Cui, Shuxian Ma*, Zhiqiang Liu, Shouhua Liu, Chen Xi, and Zhuo Cheng

Effect of freeze–thaw cycles on deformation properties of deep foundation pit supported by pile-anchor in Harbin

https://doi.org/10.1515/rams-2022-0266
received April 28, 2022; accepted August 24, 2022

Abstract: In the course of the construction of deep foundation pits during the winter in seasonally frozen areas, the pit wall soil is often unstable due to frost heave and thawing settlement, which leads to hidden safety hazards in engineering construction. Based on the analysis of the deformation data of a pile-anchor supporting a deep foundation pit in Harbin obtained from monitoring during the winter, the influence of freezing and thawing cycles was investigated. The results show that the horizontal displacement in the middle of the shallow layer of the foundation pit is significantly larger than that on both sides during the freeze–thaw cycles, and the spatial effect becomes noticeable. The stress concentration at the external corner of the foundation pit, coupled with the effects of atmospheric precipitation and freeze–thaw cycles, led to the maximum growth rate of horizontal displacement up to 1.40 mm·day^{-1}. The external corner effect is evident from 1 m in the shallow layer of the pit to the depth H/2 of the foundation pit. The support scheme is generally feasible, and we can appropriately enhance the support of the shallow layer of the foundation pit during the freeze–thaw cycles. For similar projects experiencing freeze–thaw cycles, the safety reserve can be appropriately enhanced when carrying out support design.

Keywords: seasonally frozen areas, deep foundation pit construction during winter, foundation pit monitoring, freeze-thaw cycles, external corner

*** Corresponding author: Shuxian Ma,** College of Civil Engineering, Northeast Forestry University, Harbin, 150040, China, e-mail: mashuxianya@nefu.edu.cn
Gaohang Cui, Zhiqiang Liu, Chen Xi: College of Civil Engineering, Northeast Forestry University, Harbin, 150040, China
Shouhua Liu: College of Civil Engineering, Central South University, Changsha, 410075, China
Zhuo Cheng: School of Civil Engineering and Transportation, Hebei University of Technology, Tianjin, 300131, China

1 Introduction

The soil in the seasonally frozen areas often experiences freeze–thaw cycles. Seasonally frozen soil is mainly situated in the northeast and northwest of China, North China, and other places, and the area accounts for about half of the land region [1]. As the temperature of seasonally frozen soil decreases in the winter, the soil begins to freeze. The volume of water in the soil increases by 9% during the process of freezing into ice. When more water participates in the freezing, frost heave will appear. As a result, structures buried in the soil are subjected to frost shear and frost heave forces. In the spring, as the temperature rises, ice crystals in the soil melt, resulting in excessive water content of local soil, thawing subsidence of soil, and strength reduction [2–4]. Frost heave and thawing subsidence are common freezing damages in seasonally frozen areas, which severely impact the regional projects and should be prevented in advance and treated in time.

The research of a soil in a seasonally frozen area is mainly divided into the following aspects.

The first aspect is the study of basic physical and mechanical properties, such as porosity, water content, and cohesion. Many scholars such as Yang et al. [5], Wang et al. [6], Qi and Ma [7], and Wang et al. [8] studied the effects of freeze–thaw cycles on the basic physical and mechanical properties of cohesive soils. Xiao et al. [9–11], Ni and Shi [12], Zhang et al. [13], Xu et al. [14–16], and many other scholars explored the influence of freeze–thaw cycles on the basic physical and mechanical properties of loess. Zhu [17] used lime to reinforce the soil of the low embankment on the Songnen Plain, and found that under the conditions of freeze–thaw cycles, the best lime blending ratio is 5–7%, which can effectively increase the strength while reducing the frost heave. Wang et al. [18] used the layered compaction method to prepare soil samples. Through the analysis of the results of triaxial tests, they summarized the variation rules of cohesion and

internal friction angle under freeze–thaw cycles. They proposed the correction coefficients for cohesion and internal friction angle under freeze–thaw cycles in seasonally frozen areas.

Second, the constitutive relationships of seasonally frozen soil were explored, by considering consolidation, creep, and rheology, and constitutive models were established. Scholars such as Zhu [19,20] and Zheng et al. [21] conducted indoor experiments and found that small changes in the internal temperature in the "high temperature" range (above −2.0°C) can cause drastic changes in the compressibility. Yang et al. [22] conducted tests on a high-temperature frozen soil (temperature of −1.5 to 0°C) to explore its creep characteristics, and verified that the Burgers viscoelastic model can describe the creep characteristics of the frozen soil more accurately. The multi-factor coupled constitutive model currently represents an important research direction [23], and Li et al. [24,25] used the principle of energy and mass conservation along with the Clausius–Clapeyron equation to establish a coupled heat-water-deformation model for frozen soil. Zhou and Li [26] established a thermal-hydro-mechanical coupling model of a saturated soil based on Clapeyron equation, and also used the separation porosity to judge the formation of ice lenses. Yao and Michalowski [27] established an elastoplastic constitutive model that can simulate the freezing and melting of a soil. The difference between this and the other thermo-hydro-mechanical models is that this model uses a porosity function to describe the frost heave of the soil, and the experimental data were used to verify its accuracy. Li et al. [28] used the principle of the conservation of energy and mass to derive a thermo-hydro-mechanical mathematical model, and verified it with experiments.

Third, the engineering properties of soil in seasonally frozen areas were surveyed. Wang et al. [29] monitored the temperature of the subgrade in a heavy freezing area, and studied and explained the mechanism of the frost heave of the subgrade in a seasonally frozen area. Zhou and Li [30] and Pei [31] used the Clausius–Clapeyron equation to establish a frost heave mathematical model considering temperature, displacement, and porosity. Mao et al. [32] conducted the real-time monitoring of the internal temperature and moisture of the subgrade on the section of the Jine Highway in Heilongjiang Province, and analyzed the law of water and heat changes and the causes of subgrade frost heave and frost. Bai et al. [33] established a thermo-hydro-mechanical numerical model, used water content to judge the formation of ice lenses, and explained the frost heave mechanism under complex freezing paths. Zhang et al. [34] monitored the displacement during the excavation of a deep foundation pit in soft soil. It is found that the surface subsidence calculated by the method of Hsieh and Ou is consistent with the field monitoring data and can well describe the general trend of surface subsidence. Shi et al. [35] monitored deep foundation pits supported by piles and anchors in the northwest region. Through the analysis of monitoring data, it is found that under the condition of natural frost heave in winter, the frost heave effect is most significant at the upper 0.5 m of the supporting pile. Soil frost heaving will greatly increase the internal force of retaining piles and the deformation of the superstructure. Li [36] monitored the horizontal displacement and groundwater level while constructing a super deep foundation pit. The results show that the changing trend of the axial force of the first layer anchor cable with time is consistent with the change rule of the horizontal displacement with time.

At present, research on frozen soil engineering in China is mainly concentrated on highway and railway engineering in high-latitude and high-altitude areas. There are relatively few studies on the foundation pit engineering in seasonally frozen areas, and this work mainly studies the deep foundation pits in such areas. While ensuring the safety of the project, the monitoring data were analyzed to study the changes in displacement, spatial effect, and external corner effect of the foundation pit support system during the soil freezing and thawing. The design recommendations for deep foundation pits in seasonally frozen areas during the winter are provided.

2 Overview of the foundation pit project

The project shown in this article was located in Harbin, Heilongjiang Province. Harbin is the capital city in the northernmost part of China. It is located between 125°42′–130°10′ east longitude and 44°04′–46°40′ north latitude. The summer is short and the winter is long. The winter lasts from early November to April, which is a typical freezing season, and the daily average temperature is below 0°C for nearly 150 days. Thus, the temperature roughly range from −35 to 35°C, meaning that the temperature difference reaches 70°C. At the same time, wind, snow, and rain in the high-cold area are common. Wind and water erosion cause great damage to the foundation pit support works. The winter temperatures and precipitation information of Harbin for the past 10 years are shown in Tables 1 and 2.

It can be seen from Tables 1 and 2 that since the winter begins in Harbin every November, the temperature

Table 1: Monthly average temperatures (°C) in Harbin in the winter for the period from 2011 to 2020

Years	January	February	March	April	November	December
2011	−20.9	−11.4	−3.1	7.4	−3.5	−14.1
2012	−18.2	−12.3	−3.4	7.8	−5.2	−19.4
2013	−21.0	−16.4	−7.4	4.3	−2.6	−14.1
2014	−18.4	−15.4	−1.0	10.3	−1.9	−16.8
2015	−15.7	−11.1	−1.3	8.7	−5.0	−14.0
2016	−19.3	−11.8	0.2	7.9	−9.4	−13.3
2017	−16.5	−11.0	−1.7	9.2	−5.7	−17.0
2018	−19.4	−16.1	−3.6	9.0	−2.9	−12.9
2019	−13.1	−9.2	0.2	8.5	−5.0	−15.6
2020	−16.9	−11.4	−1.1	7.5	−3.3	−15.2

Note: These data come from the Harbin (airport) weather station.

begins to drop. January of the following year is the month with the lowest average temperature, with the daily minimum temperature reaching −35°C. The temperature begins to rise in February, but the overall temperature is still low. The average temperature in April is above 0°C, the daily maximum temperature can reach 20°C, but there are still times when the temperature is below 0°C. Months with heavier precipitation are November, March, and April. In December and January, when the winter temperature is lower, the weather is relatively dry and the precipitation is also small.

A comprehensive analysis of the temperature and precipitation in the winter shows that in November each year, when the temperature drops below zero, the water in the soil begins to freeze. At the same time, when the amount of precipitation is larger, the water content of the soil near the surface increases, and the water involved in freezing is higher. In these cases, frost heave occurs in the soil. In March and early April of the following year, the temperature fluctuates around 0°C repeatedly every day, and the temperature difference between day and night is large. When the temperature is high during the day, the frozen soil and snow melt, the precipitation is large, and the water content in the soil sharply increases. At night, the temperature is low and the moisture freezes again, the soil undergoes freeze–thaw cycles, and its strength and rigidity are reduced. Therefore, the displacement monitoring during these two periods is very important.

2.1 Project overview

The deep foundation pit project was located in the prosperous business district of Harbin. The excavation depth was 20.6–23.2 m; the length was 186 m; and the width was 120 m. The total amount of excavation was about 310,000 m^3. The transportation around the foundation pit was convenient, such that the east, south, and north sides were adjacent to the roads, and the west side was adjacent to 7-story residential buildings. There were no high-rise and super high-rise buildings around the foundation pit,

Table 2: Total monthly precipitation (mm) in Harbin from 2011 to 2020

Years	January	February	March	April	November	December
2011	3.3	4.3	6.1	26.0	12.0	0.8
2012	0.0	1.7	20.0	33.0	32.0	13.0
2013	2.1	15.0	8.1	11.0	18.0	3.6
2014	0.8	1.2	1.0	6.0	1.2	11.0
2015	0.8	16.0	2.1	6.2	4.9	18.0
2016	2.3	2.9	10.0	16.0	32.0	1.9
2017	4.5	5.0	4.9	2.7	6.6	5.9
2018	6.2	4.1	11.0	26.0	16.0	4.5
2019	1.8	0.0	12.0	18.0	12.0	29.0
2020	7.0	18.0	14.0	13.0	62.0	0.7

Note: These data come from the Harbin (airport) weather station.

Table 3: Supporting structure of the foundation pit

Position	East side	South side	West side	North side
Support form	Upper steel sheet pile Lower pile anchor support	Upper steel sheet pile Lower pile anchor support	Upper pile anchor support Lower steel sheet pile	Single pile anchor support
Crown beam position	6 m underground	6 m underground	1 m underground	1 m underground

whereas there were underground shopping malls on the north and east sides.

The surrounding buildings and engineering conditions around the foundation pit were different, and the supporting levels were also different. The nearest residential building on the west side was only 4 m away. In general, the excessive soil deformation or failure of a supporting structure seriously affect the safety of the surrounding buildings, meaning that the safety level of the foundation pit should be a top priority. The supporting structure of the entire foundation pit is described in Table 3, and the supporting forms on the east and west sides of the foundation pit are shown in Figure 1.

2.2 Geological conditions

The foundation pit was located in a plain with a flat landform. The soil at the construction site was mainly composed of deposits. The specific composition of the soil is shown in Table 4. Groundwater was present at the construction site, and its level was deeply affected by the change in Songhua River water level. The annual change range was about 2–3 m. The first water level was 25.7–27.5 m underground, and the stable water level was 24.8–27.0 m underground.

2.3 Monitoring arrangement

The scale of the foundation pit project was large and the excavation depth exceeded 5 m. Since it was in the freezing area and the season was severely cold, the foundation pit monitoring was combined with local engineering experience. The north, east, and south sides of the foundation pit were adjacent to the roads. The adjacent residential buildings were only 4 m away from the nearest part of the foundation pit. Generally, the excavation and construction of foundation pits affect the settlement of surrounding buildings and roads. Thus, the surrounding buildings and roads were also monitored, except for the foundation pit itself. The specific monitoring quantities and the number of monitoring points are shown in Table 5, whereas the specific layout of the monitoring points is shown in Figure 2.

3 Analysis of the monitoring results

The winter in Harbin lasts from the end of October to the end of April. The frost heave period lasts from the end of October to the end of February, whereas the freeze–thaw cycle period lasts from the beginning of March to the end

(a) (b)

Figure 1: Supporting diagram of the foundation pit. (a) East side and (b) west side.

Table 4: Composition of the soil layers

Layer number	1	2	3	4	5	6	7	8
Type of soil layer	Miscellaneous fill	Silty clay	Silty clay	Silty clay	Silty clay	Medium sand	Coarse sand	Gravel sand
Layer thickness (m)	3.0	2.0	6.5	5.0	6.5	2.0	7.0	4.0
Weight ($kN \cdot m^{-3}$)	15.0	19.6	19.2	19.6	19.4	19.5	21.0	21.5

of April. In this work, mainly the data of winter monitoring were analyzed.

3.1 Monitoring and analysis of the steel sheet pile top horizontal displacement

The support forms on the east and south sides were both the upper steel sheet pile support and the lower pile anchor support. The adopted steel sheet pile had the I36 section, with a total length of 16 m and an embedded depth of 10 m. A total station was used to monitor the horizontal displacements. The measuring points on the top of the steel sheet pile were GB1–13, and the displacement-time diagrams for each measuring point were drawn according to the obtained data. The displacement-time diagrams at the measuring points GB2–GB5 were used to reflect the change in the steel sheet pile top horizontal displacement on the east side, whereas the displacement-time diagrams at the measuring points GB7, GB9, GB10, and GB12 were used to reflect the change in the south side. The results are shown in Figure 3.

In Figure 3, the displacement changes in time were roughly divided into three stages.

The first stage lasted from November 11 to December 26, and represents the excavation stage of the foundation pit. It can be seen from Figure 3 that the displacement in this stage linearly increased in time, and that the horizontal displacement and change trend at each measuring point on the steel sheet pile top were basically the same. The displacements at the measuring points GB4 (in the middle of the east side) and GB10 (in the middle of the south side) were relatively large, with a maximum of 5 mm, and the horizontal displacement growth rate was $0.11\ mm \cdot day^{-1}$. Minimum displacement at the measuring points GB5 and GB9 located next to GB4 and GB10 was 3 mm, and the horizontal displacement growth rate was $0.07\ mm \cdot day^{-1}$.

The second stage lasted from December 27 to February 24 of the following year. It was the vacant stage of the steel sheet piles in the foundation pit. During this time, the horizontal displacement at each measuring point basically remained stable. Horizontal displacements at the measuring points GB4, GB9, and GB10 did not change, the horizontal displacement increment at the measuring point GB3 was 1 mm, and the horizontal increment at the measuring points GB2, GB5, GB7, and GB12 was 2 mm. It can be seen from Figure 1 that during this stage the temperature in Harbin was the lowest throughout the year, i.e., it was always below 0°C, but the freezing of the soil had no effect on the horizontal displacement of the steel sheet pile top.

Tests showed that as long as the content of powder and clay particles (with a particle size of less than 0.05 mm) in the coarse-grained soil was controlled within the range of 5%, the frost heave did not occur. The soil layer on the upper part of the foundation pit was miscellaneous fill with loose structure, low water content, large particle size, and almost no powder and clay particles. There was little water involved in freezing, and frost heave did not occur. At the same time, heat preservation measures were taken on the side walls of the foundation pit, which effectively reduced the impact of the low temperature environment on the steel sheet pile top horizontal displacement.

The third stage lasted from February 25 to April 25. During this stage, the steel sheet piles of the foundation pit were still in the vacant stage. The horizontal displacement of the top of the steel sheet piles linearly increased in time, and the growth rate was larger than that of the first stage. The maximum horizontal displacement at the measuring point GB10 was 28 mm, the horizontal displacement increment accounted for 82.14% of the displacement obtained during the whole winter, and the horizontal displacement growth rate was $0.38\ mm \cdot day^{-1}$. The minimum horizontal displacement at the measuring point GB7 was 22 mm, the displacement increase was 16 mm, and the horizontal displacement increase rate was $0.27\ mm \cdot day^{-1}$. It can be seen from Table 1 that during this period, the temperature in Harbin during the day was above 0°C. Snow melting on the ground surface penetrated into the foundation pit soil through the cracks in the surrounding road surface, and the lower frozen soil was not completely melted, causing the water content of the upper soil body to be sharp. Then, due to more water involved in freezing, the soil heave occurred. At the same time, the temperature difference between day and night was large, the soil

Table 5: Monitoring project and the number of measuring points

Monitoring project	The surface settlement of the road	Horizontal displacement of the retaining pile top	Deep horizontal displacement of the foundation pit	Anchor cable tension	Horizontal displacement of the steel sheet pile top
Number of measuring points	34 (ZB1–ZB34)	34 (GL1–GL34)	15 (KB1–KB15)	19 (M1–M19)	13 (GB1–GB13)

was in the state of freeze–thaw cycle, its stiffness decreased, resulting in a large increase in the steel sheet pile top horizontal displacement.

3.2 Monitoring and analysis of the crown beam top horizontal displacement

Due to the different adjacent buildings and structures around the foundation pit, different support forms were adopted on four sides of the foundation pit, and the positions of the crown beams were also different. On the east and south sides of the foundation pit, the crown beam was located 6 m underground, and on the west and north sides, it was located 1 m underground. The total station was used for the monitoring of horizontal displacements, the measuring points GL1–34 were placed on the crown beam top, and the displacement-time diagrams for each measuring point were also determined according to the monitoring data. Among them, the displacement-time diagrams of the measuring points GL1, GL3, and GL6 reflected the changes in horizontal displacements on the east side, whereas the measuring points GL7, GL9, and GL11–13 corresponded to the south side. The measuring points GL16–19 were related to the west side, and the measuring points GL26, GL27, GL29, and GL32 corresponded to the north side. The displacement changes are shown in Figure 4.

It can be seen from Figure 4 that in the winter time period in Harbin, the displacements of the east, south and west sides of the foundation pit varied in time, and that the trend is similar to that of the horizontal displacement of the steel sheet pile top. The horizontal displacement trend of the north side only had a linear upward phase, because the excavation of the foundation pit was to be carried out only after the year, and the north side was in the excavation deformation stage until April 25.

In the east, south and west sides of the foundation pit, the horizontal displacements of the crown beam tops on the east and west sides were larger, and the displacement on the west side was smaller. The horizontal displacement at the measuring point GL3 on the east side of the foundation pit significantly increased after March 11. On March 26, the horizontal displacement increased by 145.45%, and the horizontal displacement growth rate was 1.07 mm·day^{-1}. This is because the continuous rainfall in Harbin during this period, the water content of the soil in the foundation pit increased, the cohesion and the angle of internal friction decreased, the strength and stiffness of the soil decreased as well, and the horizontal

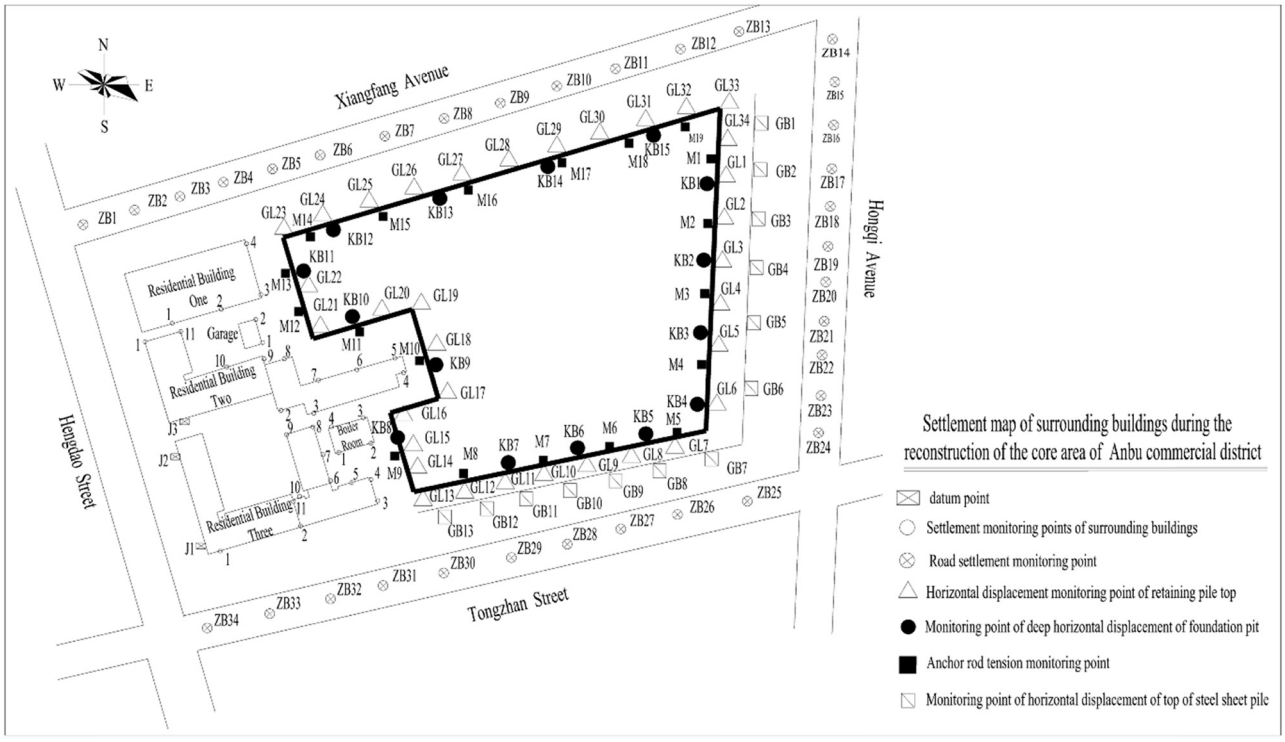

Figure 2: Layout of the monitoring points.

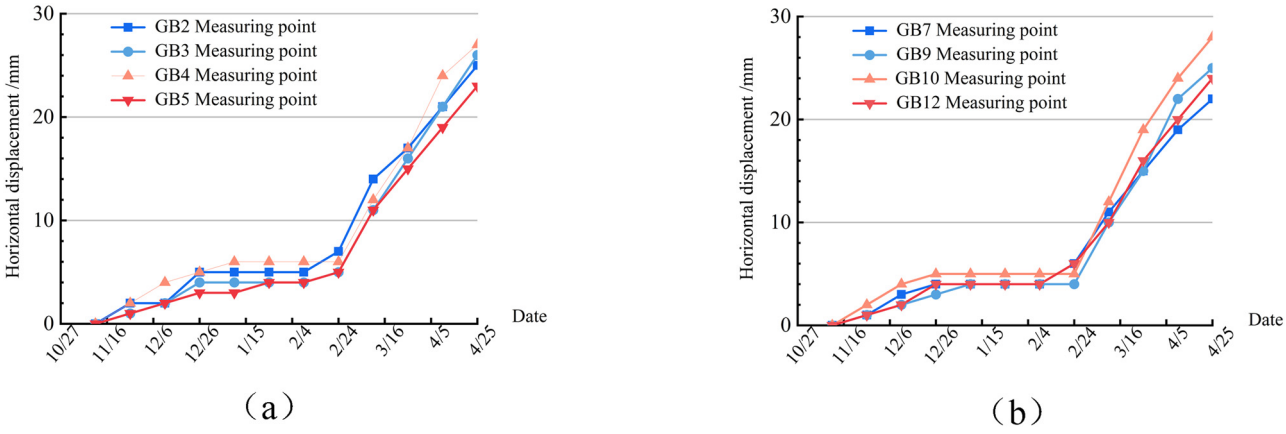

Figure 3: Horizontal displacement diagrams of the steel sheet pile top. (a) East side and (b) south side.

displacement of the soil significantly increased. Before February 24, the horizontal displacement and increment at the measuring points GL7 and GL9 on the south side of the foundation pit were small, the maximum increment reached 120% on March 11, and the maximum horizontal displacement growth rate was 0.40 mm·day^{-1}, and the crown beam was close to the ground (i.e., 1 m underground). Therefore the attention was given to the horizontal displacement of several other measuring points on the south side on March 26. The horizontal displacement trend at the measuring points GL11–13 was basically the same as that of other measuring points. The west side of the foundation pit was adjacent to residential buildings, and the nearest was only 4 m away. The measuring point GL18 was set there, the measuring points GL17 and GL19 were set up at the external corners, and the measuring points GL16 and GL21 were set up at the internal corners. Before February 24, the horizontal displacement and change trend at the measuring points on the west side were basically the same. Afterwards, due to the large temperature difference between day and night, the soil experienced freeze–thaw cycles, and its strength and

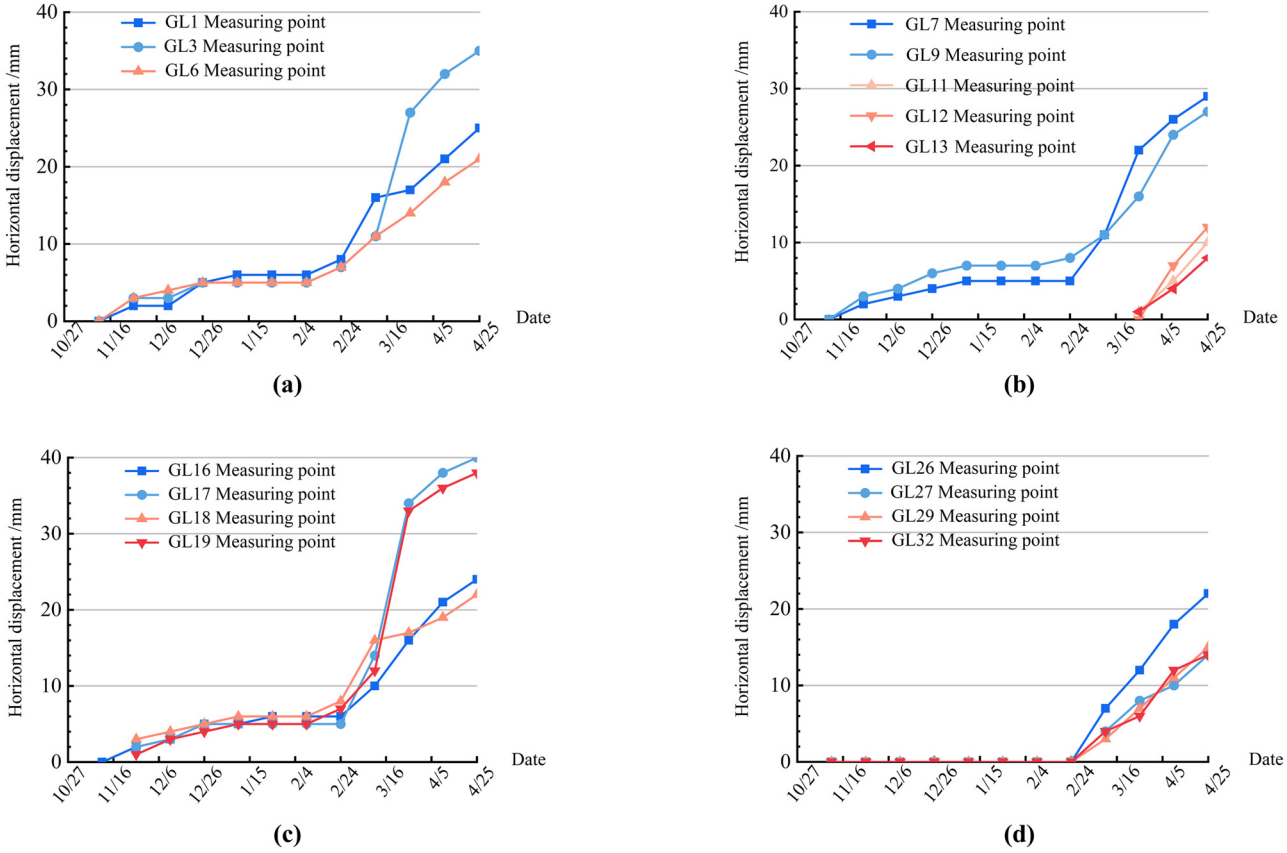

Figure 4: Horizontal displacement diagrams of the crown beam top. (a) East side, (b) south side, (c) west side, and (d) north side.

stiffness were reduced, resulting in an increase in the horizontal displacement of the crown beam top. Since the continuous rainfall on March 11, the horizontal displacement at the measuring point on March 26 increased by up to 175%, and the maximum horizontal displacement growth rate was 0.40 mm·day^{-1}. At the same time, the stress concentration at the external corner caused the most obvious increase in the horizontal displacement at the measuring points GL17 and GL19, and the maximum horizontal displacement growth rate was 1.40 mm·day^{-1}.

Since the excavation of the northern part of the foundation pit was carried out only the year later, the monitoring of the horizontal displacement of the crown beam top on the north side of the foundation pit began on February 24. During this period, the soil was in the state of freeze–thaw cycles, the stiffness of the soil was greatly reduced compared with the freezing period of the winter, and the horizontal displacement and growth rate at each measuring point were relatively large. The measuring point GL26, which was located in the middle of the north side of the foundation pit, had the largest horizontal displacement.

3.3 Monitoring and analysis of the supporting structure's deep horizontal displacement

In addition to the monitoring of the horizontal displacements of the supporting structure top, the deep horizontal displacement of the supporting structure was also monitored. The displacement at the measuring point KB1–7 was monitored in time to reflect the horizontal displacements at 5, 15, and 20 m. The change trend is shown in Figure 5.

It can be seen from Figure 5 that during the winter construction period, the deep displacement-time diagram of the foundation pit is the same as the horizontal displacement of the top of the steel sheet pile and the top of the crown beam, and that it can be divided into three stages.

The first stage lasted from November 11 to December 26, which was the excavation stage of the foundation pit. In this stage, the displacement increased linearly in time. At 5 m depth, the maximum horizontal displacement at the measuring point KB3 was 7.52 mm, and the minimum horizontal displacement at the measuring point KB2 was 5.87 mm. At 15 m depth, the maximum horizontal displacement

at the measuring point KB1 was 9.18 mm, and the minimum horizontal displacement at the measuring point KB3 was 4.52 mm. Finally, at the depth of 20 m, the maximum horizontal displacement at the measuring point KB1 was 9.83 mm, and the minimum horizontal displacement at the measuring point KB2 was 7.29 mm. It can be clearly seen from Figure 5 that most of the deep horizontal displacement of the foundation pit was generated during the excavation stage. The largest horizontal displacement at this stage, at the depth of 15 m, was observed at the measuring point KB1, and accounted for 85.16% of the total horizontal displacement at the end of the winter. The lowest, which was also at the depth of 15 m, was observed at the measuring point KB3, and accounted for 68.07% of the total horizontal displacement at the end of the winter.

The second stage lasted from December 27 to February 24 of the following year, which was the winter period. At this time, the east and south sides of the foundation pit were excavated to the bottom, and the horizontal displacement of each measuring point basically remained stable with a small increase. At the depth of 5 m, the maximum horizontal displacement increment at the measuring point KB7 was 0.81 mm, and the horizontal displacement growth rate was about 0.014 mm·day^{-1}. At the depth of 15 m, the maximum horizontal displacement increment at the measuring point KB6 was 0.90 mm, and the horizontal displacement growth rate was 0.015 mm·day^{-1}. At the depth of 20 m, the maximum horizontal displacement increment at the measuring point KB5 was 0.92 mm, and the horizontal displacement growth rate was about 0.015 mm·day^{-1}. During this time, the temperature was below 0°C, so the heat preservation measures were undertaken, and the bottom of the pit was also waterproofed. In these 60 days, the maximum increase in the horizontal displacement of each measuring point did not reach 1 mm, which verified that the supporting structure and thermal insulation measures on the east and south sides of the foundation pit effectively prevented the increase in the horizontal displacement.

The third stage lasted from February 25 to April 25. It was the stage of continued excavation of the foundation pit and construction of the building foundation. The horizontal displacement of each measuring point increased linearly in time. At the depth of 5 m, the maximum horizontal displacement increment at the measuring point KB5 was 1.69 mm, which is an increase of 24.53% compared to

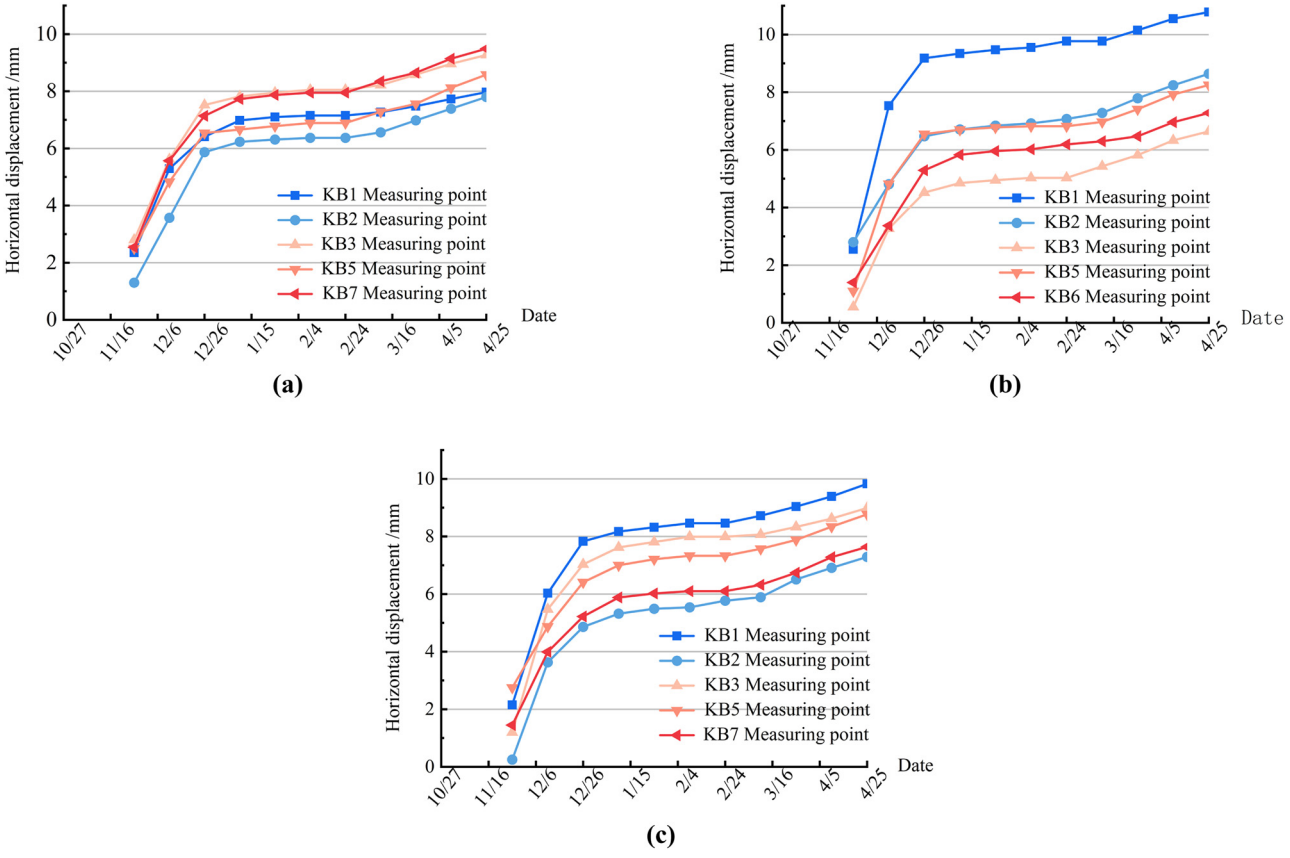

Figure 5: Horizontal displacement at different depths of the supporting structure. (a) 5 m deep, (b) 15 m deep, and (c) 20 m deep.

Table 6: UCT fitting surface parameters

Monitoring points	k_1	k_2	k_3	k_4	k_5	k_6	R^2
KB1	−1.31926	0.78421	−0.03045	0.00065	−0.00042	0.09795	0.80235
KB2	−0.79789	0.57151	−0.02487	0.00068	−0.00029	0.08222	0.83765
KB3	8.06742	−1.31203	0.0508	0.00022	−0.00036	0.09328	0.85006

the previous stage. At the depth of 15 m, the maximum horizontal displacement increment at the measuring point KB3 was 1.61 mm, with an increase of 32.01% compared to the previous stage. Finally, at the depth of 20 m, the maximum horizontal displacement increment at the measuring point KB7 was 1.54 mm, which is an increase of 25.25% compared to the previous stage. It can be seen from Table 1 that at this stage both the temperature difference between day and night and rainfall were large. The freeze–thaw cycles caused the decrease in stiffness, which increased the horizontal displacement of the foundation pit. Moreover, the rapid increase in the water content in the soil caused the rheology of the soil to increase, and the horizontal displacement of the upper part of the foundation pit was significantly affected.

3.4 Monitoring and analysis of horizontal displacement of special parts

The main road adjacent to the east side of the foundation pit is sensitive to the deformation of the foundation pit. Thus, the horizontal displacement on the east side of the foundation pit is monitored. The horizontal displacement

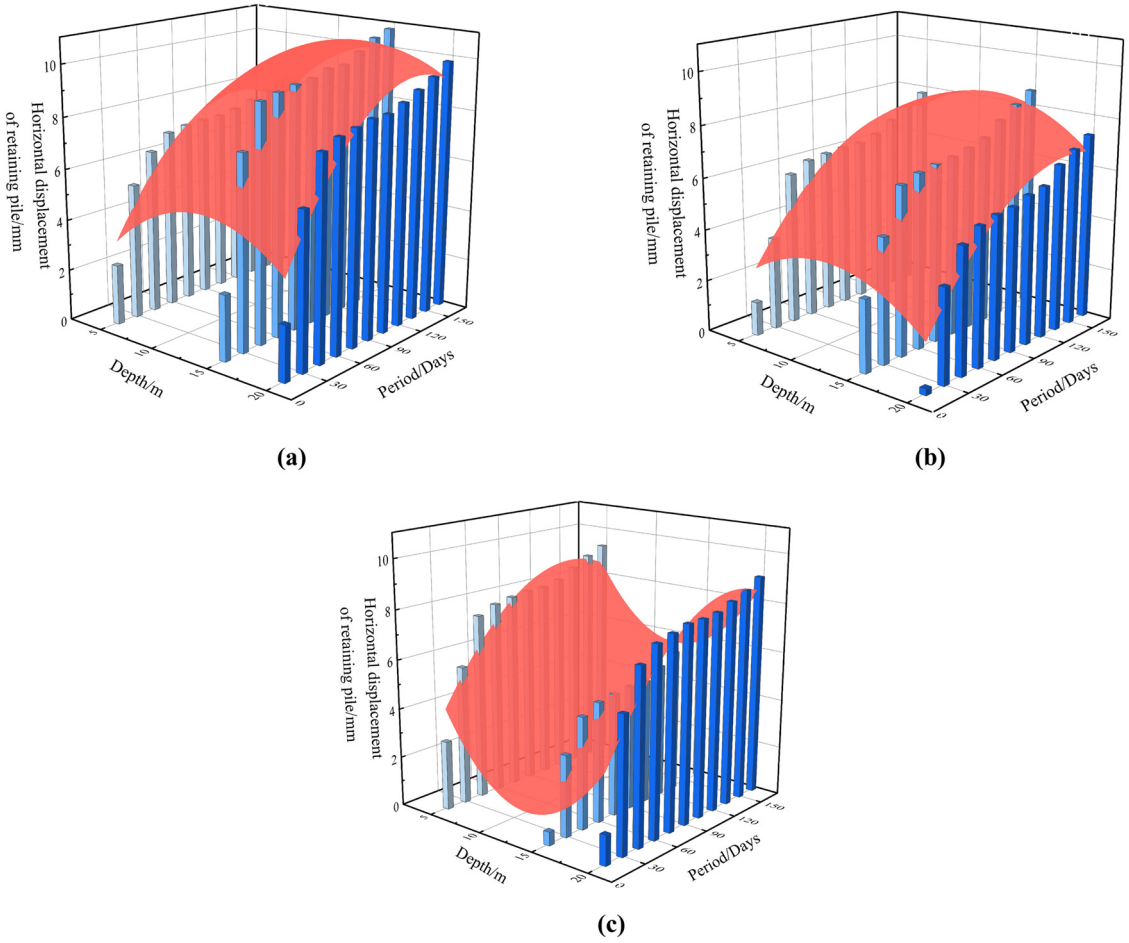

Figure 6: Horizontal displacement fitting surface of monitoring point. (a) KB1, (b) KB2, and (c) KB3.

of monitoring points at different depths on the east side is fitted every 15 days, and the following fitting formula is given:

$$X_i = k_1 + k_2H + k_3H^2 + k_4HP + k_5P^2 + k_6P, \quad (1)$$

where X_i – the horizontal displacement of the monitoring point; H – depth; and P – monitoring days.

The specific data of the fitting parameters are shown in Table 6. Taking the depth as the X-axis, the monitoring days as the Y-axis, and the horizontal displacement of the monitoring point as the Z-axis, the fitting surface in the three-dimensional space is shown in Figure 6. R^2 is greater than 0.80, and this formula has an excellent fit effect.

The pile-anchor support structure is used on the east side of the foundation pit. The KB3 monitoring point is near the prestressed anchor at a depth of 15 m, and the prestressed anchor effectively limits the horizontal displacement of the foundation pit. Therefore, the horizontal displacement of the KB3 monitoring point has a trend of first increasing, then decreasing, and then increasing with the increase in the depth. The monitoring points KB1 and KB2 are located between the anchors. The horizontal displacement of these two monitoring points increases first and then decreases with the increase in depth, then tends to be stable.

To explore the variation law of the horizontal displacement of the shallow part on the east side with time, we fit the horizontal displacement of the monitoring points on the east side at 15-day intervals. The following fitting equation is obtained:

$$X_S = -2.70045 + 0.25665D - 0.00157D^2 - 0.00058DP + 0.00158P^2 - 0.08569, \quad (2)$$

where X_S – the horizontal displacement at a depth of 1 m on the east side of the pit. D – the horizontal distance from the northern most point on the eastern side of the pit. P – the number of monitoring days.

Taking the distance as the X-axis, the monitoring period as the Y-axis, and the horizontal displacement of the monitoring point as the Z-axis, the fitted surface in three-dimensional space is made, as shown in Figure 7. The formula has an excellent fitting effect with an R^2 of 0.86747. It can be seen from Figure 7 that in the early stage of pit construction, the horizontal displacement of the shallow part in the middle of the pit is not larger than that on both sides of the foundation pit. Hence, there is no obvious spatial effect in the foundation pit. The shallow soil body experience repeated freezing and thawing cycles by March and April of the following year. At the same time, a large amount of rainfall leads to a sharp increase in the

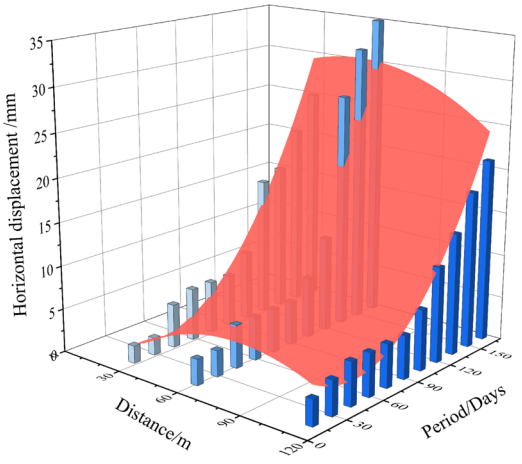

Figure 7: Horizontal displacement fitting surface of west side.

shallow water content of the foundation pit. Therefore, the horizontal displacement of the shallow part in the middle of the foundation pit increases rapidly. It is significantly greater than the horizontal displacement of the shallow part on both sides of the foundation pit. Then, the spatial effect of the foundation pit becomes apparent, and the support there can be strengthened.

The west side of the pit is adjacent to a 7-story residential building, so the shape of the foundation pit is irregular. The external corner of the foundation pit has a protruding surface of the soil on both sides, which is more sensitive to horizontal displacement and prone to local tension cracking damage, affecting the stability of the foundation pit. The horizontal displacement of the external and internal corners on this side is monitored, and the results are shown in Figure 8. The measuring point at the external corner is KB9, and the measuring point at the internal corner is KB8. At 1 m in the shallow

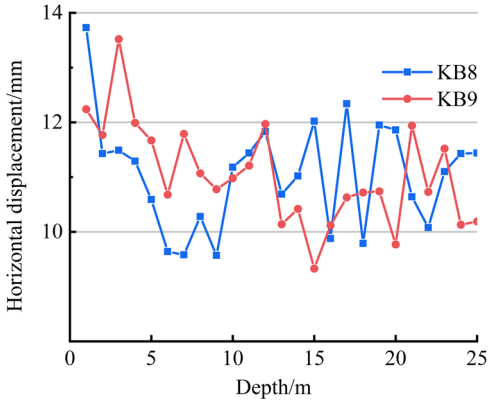

Figure 8: Horizontal displacement of external corner and internal corner.

part of the foundation pit, the horizontal displacement of the external corner is significantly smaller than that of the internal corner. The support scheme at this point effectively weakens the external corner effect. However, in the range from 1 m depth to H/2 depth of the foundation pit, the displacement of the external corner is higher than that of the internal corner, and the effect of the external corner is obvious so that the support can be strengthened in this part.

4 Conclusion

In this work, a deep foundation pit project in Harbin was monitored. Through the analysis of the monitoring results obtained during the winter, the following conclusions were drawn:

1) In March and early April, the temperature difference between day and night is large in Harbin, and the soil is under the action of freeze–thaw cycles, which damages the foundation pit soil structure, reduces the soil strength and rigidity, and ultimately causes the horizontal displacement of the foundation pit soil to increase rapidly in time.
2) When the temperature in the seasonally frozen areas rises, the snow melts and penetrates into the foundation pit soil along the road cracks. The lower soil has not yet melted, resulting in a sharp increase in the upper soil's water content, and the nature of the soil becomes unstable. Attention should be paid to the drainage of the foundation pit to prevent the instability of the soil properties caused by snow melting.
3) The shallow soil repeatedly experiences the freeze–thaw cycle in late winter and early spring. The horizontal displacement of the shallow part in the middle of the foundation pit is significantly larger than the horizontal displacement of the shallow layer on both sides of the foundation pit – the spatial effect of the foundation pit changes from inconspicuous to obvious. We can strengthen the support of the shallow layer of the foundation pit to reduce the spatial impact of the foundation pit.
4) From the shallow layer of the foundation pit 1 m to the depth of the pit H/2, the external corner effect is obvious, and the safety reserve can be increased appropriately when carrying out the support design.

Acknowledgments: This work was supported by the Fundamental Research Funds for the Central Universities (DL12CB03); National Natural Science Foundation of China (50538030); and Natural Science Foundation of Heilongjiang Province (E201149).

Funding information: Fundamental Research Funds for the Central Universities (DL12CB03); National Natural Science Foundation of China (50538030); and Natural Science Foundation of Heilongjiang Province (E201149).

Author contributions: Gaohang Cui: resources, writing – review and editing; Shuxian Ma: writing – original draft; Zhiqiang Liu: investigation; Shouhua Liu: methodology; Chen Xi: data curation; Zhuo Cheng: supervision.

Conflict of interest: The authors declare that they have no known competing financial interests or personal relationships that could have appeared to influence the work reported in this article.

References

[1] Xu, X. Y., and M. G. Qiu, Eds. *Advanced soil mechanics*. Harbin Institute of Technology, HL, Harbin, 2008.
[2] Cui, G. H., S. H. Liu, Z. L. Wang, and R. J. Zhang. Research on engineering monitoring of a pile-anchor-supported deep foundation pit in Harbin under frost heave environment. *Journal of Engineering Geology*, Vol. 24, No. 2, 2016, pp. 331–338.
[3] Cui, G. H., S. H. Liu, Z. L. Wang, and R. J. Zhang. Monitoring of a pile-anchor supporting deep foundation pit project in Harbin. *Journal of Building Structures*, Vol. 37, No. 7, 2016, pp. 144–150.
[4] Liu, S. H. Research on safety of deep foundation pit supported by pile-anchor in a certain winter in Harbin. Master's dissertation. Northeast Forestry University, Harbin, 2016.
[5] Yang, C. S., P. He, G. D. Cheng, Y. L. Zhu, and S. P. Zhao. Experimental study on the influence of freezing and thawing on soil dry bulk density and water content. *Chinese Journal of Rock Mechanics and Engineering*, Vol. 22, No. 2, 2003, pp. 2695–2699.
[6] Wang, D. Y., W. Ma, X. X. Chang, W. J. Feng, and J. W. Zhang. The effect of freeze-thaw cycles on the physical and mechanical properties of Qinghai-Tibet clay. *Chinese Journal of Rock Mechanics and Engineering*, Vol. 24, No. 23, 2005, pp. 4313–4319.
[7] Qi, J. L. and W. Ma. The influence of freezing and thawing on the strength of over consolidated soil. *Chinese Journal of Geotechnical Engineering*, Vol. 28, No. 12, 2006, pp. 2082–2086.
[8] Wang, D. Y., W. Ma, Y. H. Niu, X. X. Chang, and Z. Wen. Effect of cyclic freezing and thawing on mechanical properties of Qinghai-Tibet clay. *Cold Regions Science and Technology*, Vol. 48, No. 1, 2007, pp. 34–43.

[9] Xiao, D. H., W. J. Feng, and Z. Zhang. Porosity changes of loess under freeze-thaw cycles. *Journal of Glaciology and Geocryology*, Vol. 36, No. 4, 2014, pp. 907–912.
[10] Xiao, D. H., W. J. Feng, Z. Zhang, J. Ming, and Q. Wang. The influence of freeze-thaw cycles on the permeability changes of Lanzhou loess. *Journal of Glaciology and Geocryology*, Vol. 36, No. 5, 2014, pp. 1192–1198.
[11] Xiao, D. H., W. J. Feng, Z. Zhang, and J. Ming. Study on the relationship between permeability and structural characteristics of loess under freeze-thaw cycles. *Hydrogeology and Engineering Geology*, Vol. 42, No. 4, 2015, pp. 43–49.
[12] Ni, W. K. and H. Q. Shi. The effect of freeze-thaw cycles on the microstructure and strength of loess. *Journal of Glaciology and Geocryology*, Vol. 36, No. 4, 2014, pp. 922–927.
[13] Zhang, H., T. X. Wang, and Y. Luo. Study on the freeze-thaw strength of unsaturated undisturbed loess. *Journal of Northwest Sci-Tech University of Agriculture and Forestry* (*Natural Science Edition*), Vol. 43, No. 4, 2015, pp. 210–222.
[14] Xu, J., Z. Q. Wang, J. W. Ren, and J. Yuan. Experimental analysis on the seepage law of remodeled loess under freezing and thawing conditions. *Journal of Northwest Sci-Tech University of Agriculture and Forestry* (*Natural Science Edition*), Vol. 45, No. 7, 2017, pp. 134–142.
[15] Xu, J., Z. Q. Wang, J. W. Ren, and J. Yuan. Experimental study on the shear strength degradation characteristics of remodeled loess during freezing and thawing. *Journal of Xi'an University of Architecture and Technology* (*Natural Science Edition*), Vol. 49, No. 2, 2017, pp. 200–206.
[16] Xu, J., Z. Q. Wang, J. W. Ren, and J. Yuan. Comparative experimental study on permeability characteristics of undisturbed and remolded loess during freezing and thawing. *Journal of Engineering Geology*, Vol. 25, No. 2, 2017, pp. 292–299.
[17] Zhu, F. Research on Lime Soil Reinforcement Mechanism and Application of Low Embankment in Seasonal Frozen Area of Songnen Plain. Master's dissertation. Jilin University, Jilin, 2016.
[18] Wang, M., S. J. Meng, X. M. Yuan, Y. Q. Sun, J. Zhou, X. B. Yu, et al. Research on the freeze-thaw correction coefficient of the typical soil shear strength in seasonal frozen area. *Chinese Journal of Rock Mechanics and Engineering*, Vol. 37, No. 1, 2018, pp. 3756–3764.
[19] Zhu, Y. L. and J. Y. Zhang. Elastic deformation and compression deformation of frozen soil. *Glaciology and Geocryology*, Vol. 4, No. 3, 1982, pp. 29–40.
[20] Zhu, Y. L., Y. Z. Liu, and X. D. Xie. Field creep test study of underground ice on the Qinghai-Tibet Plateau. *Collection of Qinghai-Tibet Frozen Soil Research Papers*, Science Press, Beijing, 1983, pp. 124–130.
[21] Zheng, B., J. M. Zhang, X. J. Ma, and J. W. Zhang. Research on compression deformation characteristics of high temperature and high ice content frozen soil. *Chinese Journal of Rock Mechanics and Engineering*, Vol. 28, No. 1, 2009, pp. 3063–3069.
[22] Yang, S. Q., N. N. Wang, and H. Zhang. Study on creep characteristics and creep model of high-temperature frozen soil. *Glaciology and Geocryology*, Vol. 42, No. 3, 2020, pp. 834–842.
[23] Chen, Z. H. and N. Guo. New progress in the study of unsaturated soil and special soil mechanics and engineering applications. *Rock and Soil Mechanics*, Vol. 40, No. 1, 2019, pp. 1–54.
[24] Li, N., B. Chen, F. X. Chen, and X. Z. Xu. The coupled heat-moisture-mechanic model of the frozen soil. *Cold Regions Science and Technology*, Vol. 31, No. 3, 2000, pp. 199–205.
[25] Li, N., F. X. Chen, B. Su, and G. D. Cheng. Theoretical frame of the saturated freezing soil. *Cold Regions Science and Technology*, Vol. 35, No. 2, 2002, pp. 73–80.
[26] Zhou, J. Z. and D. Q. Li. Numerical analysis of coupled water, heat and stress in saturated freezing soil. *Cold Regions Science and Technology*, Vol. 72, 2011, pp. 43–49.
[27] Yao, Z. and R. L. Michalowski. Thermal-hydro-mechanical analysis of frost heave and thaw settlement. *Journal of Geotechnical and Geoenvironmental Engineering*, Vol. 141, No. 7, 2015, id. 04015027.
[28] Li, S. Y., M. Y. Zhang, W. S. Pei, and Y. M. Lai. Experimental and numerical simulations on heat-water-mechanics interaction mechanism in a freezing soil – ScienceDirect. *Applied Thermal Engineering*, Vol. 132, 2018, pp. 209–220.
[29] Wang, S. J., Z. G. Chen, W. J. Qin, and L. M. Yu. Analysis of the frost heave mechanism of roadbed in seasonally frozen areas. *Highway and Transportation Science and Technology*, Vol. 29, No. 7, 2012, pp. 20–24, 44.
[30] Zhou, J. Z. and D. Q. Li. Numerical analysis of coupled water, heat and stress in saturated freezing soil. *Cold Regions Science and Technology*, Vol. 72, 2012, pp. 43–49.
[31] Pei, W. S. Study of the hydro-thermal-mechanical interaction process of frozen soil and its numerical simulation. Doctoral dissertation. University of Chinese Academy of Sciences, Lanzhou, 2015.
[32] Mao, X. S., L. Y. Wang, Z. Dawa, Z. Tsering, H. N. Zhang, W. L. Li, et al. Research on frost heave and frost boiling of subgrade caused by water and heat changes in seasonally frozen areas. *Highway*, Vol. 37, No. 1, 2017, pp. 1–5.
[33] Bai, R., Y. Lai, and Z. You. Simulation of heat–water–mechanics process in a freezing soil under stepwise freezing. *Permafrost and Periglacial Processes*, Vol. 31, No. 1, 2020, pp. 200–212.
[34] Zhang, X. H., X. C. Zhang, and H. S. Han. A case study on field monitoring analysis of deep foundation pit in soft soils. *Advances in Civil Engineering*, Vol. 2019, 2019, id. 9342341.
[35] Shi, D. M., Y. X. Li, X. Y. Gao, S. H. Li, and X. Tian. Analysis of internal force and displacement of foundation pit pile anchor supporting structure based on soil frost heaving. *2020 2nd International Conference on Civil, Architecture and Urban Engineering, Atlanta, October 9–13, 2022*, IOP Publishing Ltd, 2020, p. 012028.
[36] Li, Z. Q. Displacement monitoring during the excavation and support of deep foundation pit in complex environment. *Advances in Civil Engineering*, Vol. 2021, 2021, id. 5715306.